Structural disorder and anomalous diffusion in random packing of spheres.

Palombo M.[1 2*], Gabrielli A.[1 3], Servedio V.D.P.[1], Ruocco G.[1 2], Capuani S.[2 4]

[1]Physics Department, Sapienza University of Rome, P.le A.Moro, 5 00185 Rome, Italy

[2]CNR IPCF UOS Roma, Physics Department, Sapienza University of Rome, P.le A.Moro,5 00185 Rome, Italy

[3]ISC-CNR, Via dei Taurini, 19 00185 Rome, Italy

[4]Center for Life Nano Science@Sapienza, Istituto Italiano di Tecnologia, Rome, Italy

*Corresponding author: marco.palombo@roma1.infn.it

Dr. Andrea Gabrielli: andrea.gabrielli@roma1.infn.it

Dr Vito Domenico Pietro Servedio: Vito.Servedio@roma1.infn.it

Prof. Giancarlo Ruocco: giancarlo.ruocco@roma1.infn.it

Dr. Silvia Capuani : silvia.capuani@roma1.infn.it

Supplementary materials

Determination of $g_2(r)$

We calculate the normalized pair correlation function as the average number of sphere centers within a radial distance $r - \Delta/2$ and $r + \Delta/2$, divided by cr^2. Δ is the thickness of the spherical shell of radius r and the constant c is fixed by imposing that asymptotically $g_2(r) \to 1$ for $r \to \infty$. Different choices of Δ within a broad range from $10^{-4}a$ to $10^{-2}a$, where a is the diameter of the obstructing spheres, led to similar results.

Geometry-based analysis

The geometric nearest neighbors number distributions (GNNd) and the local sphere density distributions (LSDd) were computed by using Voronoi tessellation. The Voronoi tessellation[1] divides the system into distinct non-overlapping regions characterized by convex polyhedra surrounding each sphere. Specifically, a Voronoi polyhedron (or cell) V_i consists of the set of points closer to the center of sphere i than any other centers. In general, there are several polyhedra V_k which share a face with V_i. The spheres corresponding to the neighboring polyhedra V_k are termed geometric neighbors of sphere i. Given the whole set of Voronoi cells which completely tile the volume, we can define a local sphere density $\phi_i = \frac{v_i}{V_i}$, where v_i is the volume of the ith sphere and V_i is the volume of its Voronoi cell. In this study, a cell-based calculation[2] of the Voronoi tessellation has been used because it is particularly well-suited for applications that rely on cell-based statistics.

Local sphere density distribution (LSDd) analysis

The variance of the LSDd, $\sigma^2_{LSDd} = \langle(\phi_i - \phi)^2\rangle$, where $\langle ... \rangle = 1/N \sum_{i=1}^{N} ...$ is the average over all the N obstructing spheres, for all the simulated disordered systems as a function of the global sphere packing, ϕ, is reported in **Fig.S1**.

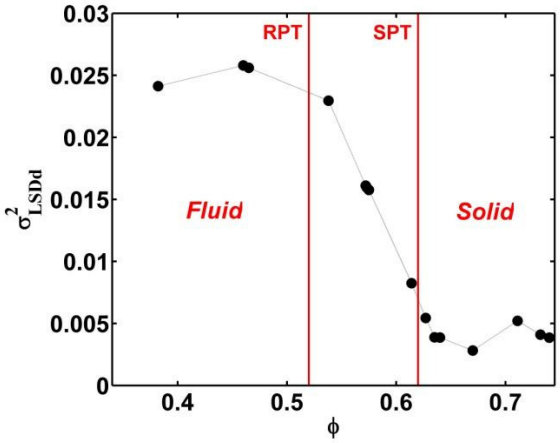

Fig. S1 Variance of the local sphere density distribution, σ^2_{LSDd}, as a function of the global sphere packing ϕ. The rigidity and stress percolation threshold (RPT and SPT respectively) are also shown as red straight lines in order to discriminate the structural state of all the simulated systems. The decrease of σ^2_{LSDd} value is indicative of an increase in structural order.

From this figure, we notice that densely packed systems exhibit smaller fluctuations in their local volume fraction than more loosely-packed ones. For dense systems, the decrease in fluctuations of local ϕ is suggestive of a decreasing number of accessible configurations as the systems approaches random close packing (i.e.ϕ~0.640). This behavior can be related to the onset of cooperative

effects and a possible structural transition[3], which is clearly observable in **Fig.S1**. Naturally, for a perfect crystal system the fluctuations of local ϕ are null.

Average number of contacts, n_c, analysis

A deeper analysis of the local packing configurations can be performed by computing the average number of spheres in contact with any given sphere, n_c. This is the most investigated parameter in the literature on sphere packing and a precise estimate for the actual number of spheres in contact can be inferred from the behavior of the average number of neighbors, $n_t(r)$, as a function of the radial distance, r (shown in **Fig.S2**). In the ideal case of identical packed spheres, one would expects that $n_t(r)$ has a discontinuity at $r = a$, where a is the diameter of the spheres, from zero to the number of neighbors in contact n_c, followed by some kind of growth for $r > a$. In **Fig.S2** the step-like behavior of $n_t(r)$ at $r = a$ for the simulated systems is clearly shown. Moreover, from all the simulated systems, we observed an increasing trend of the extrapolated n_c values with the packing density, as shown in the insert of **Fig. S2**.

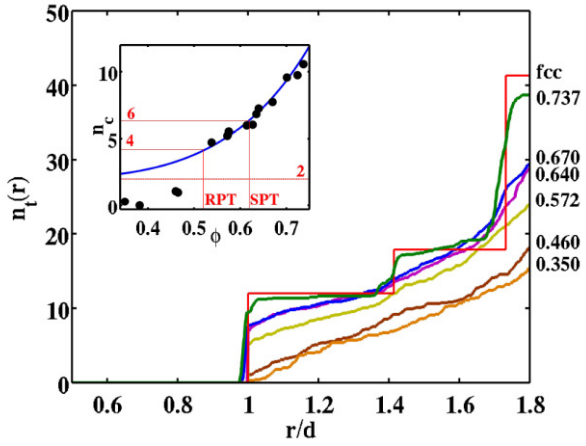

Fig. S2 The average number of neighbours, $n_t(r)$, as a function of the radial distance, r and the average number of spheres in contact with any given sphere, n_c, as a function of the sphere packing ϕ (inset). From the discontinuity of $n_t(r)$ at $r = a$ it is possible to deduce n_c as the value of $n_t(r)$ at $r = a + \varepsilon$, with $\varepsilon \to 0$. In the main plot only some $n_t(r)$ curves for the systems at the ϕ values reported on the right axis are displayed. In the inset, the extrapolated n_c values for all the simulated disordered systems are reported. Blue line represents expression (S1) fitted to the data. The extrapolation of the ϕ values at which $n_c = 4$ and $n_c = 6$ allow to estimate the RPT and SPT, respectively (red lines). The limiting value $n_c = 2$ is also displayed as a red line.

In a packing of hard spheres at mechanical equilibrium (solid-like sphere-packing system), Newton's equations for the balance of force and torque acting on each particle must be satisfied. Lagrange[4] and Maxwell[5] were the first to notice that in this kind of systems, to achieve stability, the number of degrees of freedom must balance the number of constraints. For the packing of coarse particles where the gravity is dominant, a particle should have three supporting particles underneath and in turn support other three particles, giving an $n_c = 6$. However, for the packing of particles in which the gravity force is not dominant, i.e. when friction forces are strong enough to counteract the gravity force, the densification due to sliding and rolling between particles is significantly reduced. In that case, it is understandable that the coordination number can be decreased substantially. However, to maintain the continuity in both structure and force, a minimum contact is required. Thus, it is plausible that the minimum mean coordination number is equal to 2, in order that a particle can be supported by one particle and at the same time to support another. This configuration corresponds to a chainlike packing structure. In particular, it was shown[6,7] that the balance between freedom and constraints requires $n_c = 6$ in the case of perfectly spherical frictionless spheres, and $n_c = 4$ for more realistic systems (nonspherical and/or with friction). However, there can be local configurations which contribute to n_c but do not contribute to the rigidity of the whole system or, on the other hand, there can be local arrangements which satisfy the counting rule on n_c but nevertheless are not rigid[8]. In recent years there have been theoretical approaches which consider

real, disordered, granular packing to be isostatic, i.e. free of self-induced stresses[6,9]. In a system at isostatic equilibrium, the interparticle forces are uniquely determined by the balance of force and torque alone. On the contrary, an overconstrained structure can generate self-stress and the deformation of individual particles becomes relevant. In real granular materials or in bead packs friction and rotational degrees of freedom are unavoidable, therefore the Maxwell counting[5] implies that isostatic configurations must have average connectivity of $n_c = 4$. However, in related studies for the rigidity in network glasses[10], it has been observed that there can exist two structural transitions associated with the increase of connectivity in the network: a *rigidity percolation* and a *stress percolation*, and between these two thresholds an intermediate phase which is rigid but unstressed. While the rigidity percolation occurs at the threshold predicted by Maxwell[5] ($n_c = 4$), the stress percolation transition occurs at a higher value of n_c. This suggests that sphere packings between the rigidity and the stress percolation thresholds might be in a marginal state, intermediate between fluid and solid. It is generally accepted that for the packing of monosized particles, there is a correlation between mean coordination number and sphere packing. It was found that the relationship between n_c and ϕ can be satisfactorily fitted by the following equation[11]:

$$n_c = n_c^0 \frac{1+m\phi^4}{1+n\phi^4} \qquad \text{(S1)}$$

where n_c^0, m and n are fitting parameters. Note that from the arguments mentioned above, the limiting mean coordination number n_c^0 should be equal to 2. The extrapolation from eq.(S1), fitted to the simulation data for n_c (blue solid line in the insert of **Fig.S2**), suggests that $n_c = 4$ could be reached by the system at the sphere packing $\phi \sim 0.52$ and $n_c = 6$ could be reached by the system at the sphere packing $\phi \sim 0.62$. This would place the *rigidity percolation threshold* (RPT) at the loose packing limit, according to previous works[12,13], and the *stress percolation threshold* (SPT) at the maximally random close packing. Indeed, fluid state systems having $\phi < 0.52$ show high local ϕ fluctuations, negligible geometrical frustration and $n_c < 2$; systems in marginal state, intermediate between fluid and solid, having $0.52 < \phi < 0.62$ exhibit decreasing local ϕ fluctuations, negligible geometrical frustration and $4 < n_c < 6$; finally, solid state systems having $\phi > 0.62$ exhibit low local ϕ fluctuations, increasing geometrical frustration and $n_c > 6$. In particular, for $\phi > 0.70$ one has low local ϕ fluctuations, strong geometrical frustration and $n_c \sim 10$.

Local bond orientational order parameters, Q_l, analysis

In order to establish the nature of internal organization, the bond orientational order was also calculated for all the systems. Indeed, if there is a typical disordered state or a tendency towards a specific local organization, then it is possible to associate to a given sphere packing an order parameter which measures how close the packing is to the ideal structure. As already said, it has been often argued that the competition between the tendency to form a locally compact configuration and the geometrical frustration could be the key mechanism to understand the formation of disordered packing and glassy structures. If this were the case, we would expect to see at local level configurations with rotational symmetries characteristic of icosahedral and other closed packed structures. As described in the main text, a measure of rotational symmetry which is invariant with respect to rotations in the system of coordinates is the bond orientational order Q_l, given by relation (4) of the main text. Examples of the distribution of local Q_4 and Q_6 are shown in **Fig.S3**.

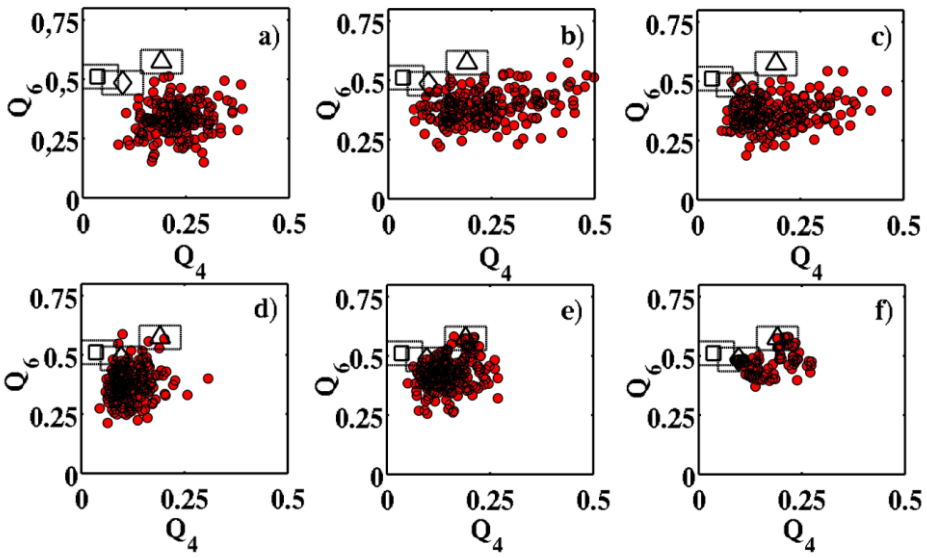

Fig. S3 Distribution of local Q_4 and Q_6 for some simulated disordered systems at different ϕ values. From **a)** to **f)** $\phi = 0.350, 0.460, 0.572, 0.640, 0.670, 0.737$. The triangles represent (Q_4, Q_6) values for the fcc crystal structure; the squares represent (Q_4, Q_6) values for the bcc crystal structure and the diamonds represent (Q_4, Q_6) values for the hcp crystal structure. The boxes surrounding the symbols representing the three characteristic crystal structures indicate the region within a range ± 0.05 from the (Q_4, Q_6) values in the corresponding ideal structures.

We observe clouds of values for Q_4 and Q_6 differently distributed around their central values $\hat{Q}_4$ and $\hat{Q}_6$. For systems at $\phi < 0.52$, the distributions of bond orientational order parameters are broad between $0.05 < Q_4 < 0.4$ and $0.2 < Q_6 < 0.5$; for systems at $0.52 < \phi < 0.62$, such distributions are narrower with $0.1 < Q_4 < 0.3$ and $0.35 < Q_6 < 0.45$, according with previous studies[12,13]; for systems at $\phi > 0.62$ we clearly observed an increasing concentration of points around values of Q_4 and Q_6 typical of closed packed structures like fcc or hcp. In order to search for signatures of known local symmetries we have measured the fraction of local configurations with values of Q_4 and Q_6 in a region within a range ± 0.05 from the values in the ideal structures fcc, hcp, and bcc (**Fig.S4**).

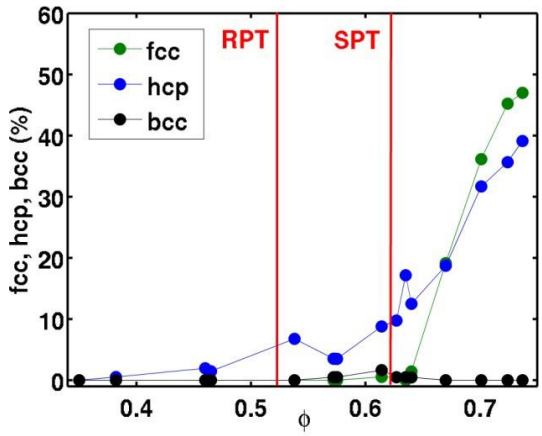

Fig. S4 Fraction of local configurations with values of Q_4 and Q_6 in a region within a range ± 0.05 from the values in the ideal structures fcc, hcp, and bcc. The net increase of fcc and hcp local configurations at $\phi > SPT$ is suggestive of an abrupt structural transition.

We found that for $\phi < 0.52$ there is a negligible fraction (<1%) of local configurations with symmetry compatible with bcc or fcc and a small fraction (between 1% to 3%) of configurations with local symmetry compatible with hcp for the systems at. For systems at $0.52 < \phi < 0.62$ we found a small fraction (between 1% to 5%) of configurations with local symmetry compatible with

bcc and fcc, and an increased fraction (between 3% to 10%) of configurations with local symmetry compatible with hcp. Finally, for systems at $\phi > 0.62$ the fraction of close packed configurations with hcp and fcc kind of local order becomes more significant at larger densities, reaching more than 30% at $\phi > 0.70$. The occurrence of a large fraction of local symmetry with an hcp-fcc-like character at $\phi > 0.62$ suggests the onset of a crystallization process that becomes relevant at $\phi > 0.70$. These findings support the idea that a tendency toward local, frustrated, icosahedral order can be responsible for the resilience to crystallize for such packings.

Geometrical frustration analysis

It has been often argued that the driving mechanism which generates amorphous structures could be the geometrical frustration. This derives from the fact that the locally most dense configuration in monosized sphere packing is achieved by placing on the vertices of an icosahedron 12 spheres in touch with a central sphere. But, icosahedral symmetry is incompatible with translational symmetry and this generates frustration: some gaps must be formed and the symmetry must be broken. Indeed, it is known that although there exist locally denser configurations, at global scale the densest achievable packings have density $\phi \leq \pi/\sqrt{18}$ which is the one of fcc and hcp crystalline configurations. We tested whether such a frustration mechanism is really relevant in our simulated systems. To this end we searched for local configurations which are locally close packed at densities larger than the crystalline ones. If a sizable amount of such configurations is found this implies that indeed the geometrical frustration must have an important role in amorphous systems. In **Fig.S5** the fraction of geometrically frustrated particles in each simulated system is reported.

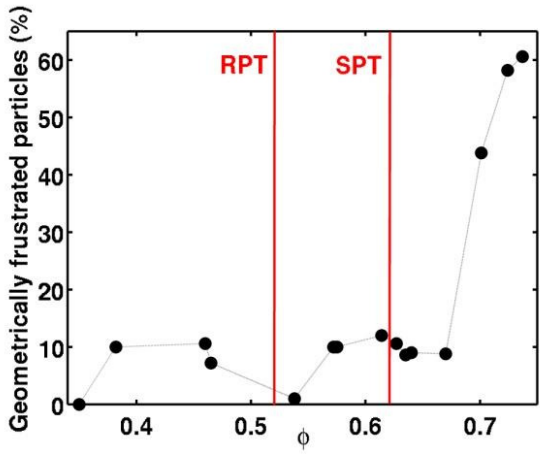

Fig. S5 Fraction of geometrically frustrated spheres for all the simulated disordered systems. RPT and SPT were also reported (red lines) in order to stress that after the abrupt structural transition at the SPT, geometrical frustration play an important role in the onset of a polycrystal structure in systems at $\boldsymbol{\phi} > 0.70$.

This result indicates that at very low values of sphere packing ($\phi < 0.52$) and also at intermediate values of sphere packing ($0.52 < \phi < 0.70$) geometrical frustration plays a negligible role in these disordered sphere packing, in agreement with previous experimental results[12,13]. Conversely, as expected, at very high values of sphere packing ($\phi > 0.70$) local sphere-arrangements with high local densities, such as the icosahedral packing, play an important role in these systems.
Local geometrical frustration is a typical characteristic of polycrystal structures[14]. Indeed, Polycrystals are globally disordered structures comprised of frustrated grains locally ordered in crystalline configurations. Due to the creation of frustrated areas between locally ordered configurations, polycrystal structures exhibit a broad spectrum of typical heterogeneity length scales. As a consequence, they are characterized by a wide distribution of voids characteristic length scales which reflects disorder properties. In **Fig.S6** we reported the variance of the size distribution of the interstitial voids, σ_{Vd}^2, as a function of the sphere packing ϕ, for all the simulated disordered systems. We found that σ_{Vd}^2 is not a monotone function of ϕ. In particular, σ_{Vd}^2 shows a local

minimum at $\phi \approx 0.62$ and increases monotonically for $\phi > 0.62$. This confirms the appearance of multiple heterogeneity length scales by frustration mechanisms and suggests, according to the CTRW framework, that in very dense amorphous packing an effective anomalous diffusion process should be observed. This means that a straight relation between the properties of structural disorder and diffusion in the hindered regime exists. As we show in the main text, unlike O_D, α embodies information about the properties of structural disorder in an effective way and allows to identify the structural transition from rigid but unstressed random jamming to stressed polycrystal structure (see **Fig.5-b** and **Fig.6** of the main text).

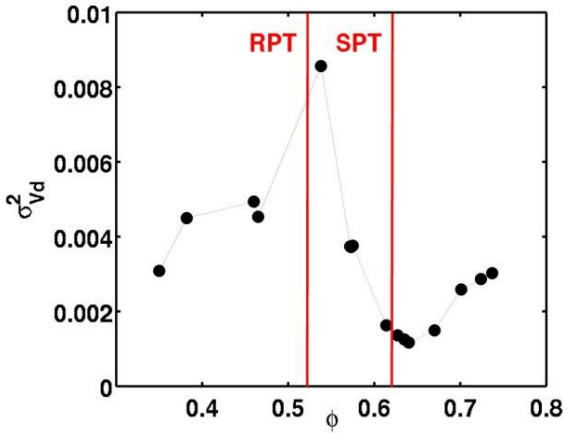

Fig S6 Variance of the size distribution of the interstitial voids, σ^2_{Vd}, as a function of the sphere packing ϕ, for all the simulated disordered systems. The non-monotonic behavior of σ^2_{Vd} as a function of ϕ is coherent with the two structural transitions identified by the two thresholds RPT and SPT (red lines), and confirms our previous results.

1. Voronoi G.F., Nouvelles applications des paramètres continus à la théorie de formes quadratiques, *J. Pure Appl. Math.* **134**, 198-287 (1908)

2. Willems T.F., Rycroft C.H., Kazi M., Meza J.C., Haranczyk M. Algorithms and tools for high-throughput geometry-based analysis of crystalline porous materials. *Micropor. Mesopor. Mat.* **149**, 134-141 (2012)

3. Schroter M., Nagle S., Radin C., Swinney H., Phase transition in a static granular system. *Euro. Phys. Lett.*. **78**, 44004-44008 (2007).

4. Lagrange J., Mecanique Analytique. (Chez la Veuve Desaint, Paris, 1788).

5. Maxwell J.C., On reciprocal figures and diagrams of forces. *Philos. Mag* **27**, 250-261 (1864).

6. Edwards S.F. and Grinev D.V., Statistical mechanics of stress transmission in disordered granular arrays. *Phys. Rev. Lett.* **82**, 5397-5400 (1999)

7. Micoulaut M., Rigidity transitions and constraint counting in amorphous networks: beyond the mean-field approach. *Europhys. Lett.* **58**, 830-836 (2002)

8. Moukarzel C.F., An efficient algorithm for two-dimensional central-force rigidity. *J. Phys. A.* **29**, 8097-8115 (1996)

9. Moukarzel C.F., Isostatic phase transition and instability in stiff granular materials. *Phys. Rev. Lett.* **81**, 1634–1637 (1998)

10. Chubynsky M.V. and Thorpe M.F., Self-organization and rigidity in network glasses. *Curr. Opin. Solid State Mater. Sci.* **5**, 525-532 (2001)

11. Yang R.Y., Zou R.P., Yu A.B., Computer simulation of the packing of fine particles. *Phys. Rev. E* **62**, 3900–3908 (2000)

12. Aste T., Saadatfar M., Sakellaiou A., Senden T.J. Investigating the geometrical structure of disordered sphere packings. *Physica A.* **339**, 16-23 (2004)

13. Aste T., Saadatfar M., Senden T.J. Geometrical structure of disordered sphere packings. *Phys. Rev. E.* **71**, 061302-061317 (2005)

14. Granasy L., Pusztai T., Borzsony T., Warren J.A., Douglas J.F., A general mechanism of polycrystalline growth, *Nature Materials* **3**, 645-650 (2004)